RJC

RASĀYAN ***J. Chem.***
Vol. 15 | No. 3 |1596-1607| July - September | 2022
ISSN: 0974-1496 | e-ISSN: 0976-0083 | CODEN: RJCABP
http://www.rasayanjournal.com
http://www.rasayanjournal.co.in

ADSORPTIVE REMOVAL OF BASIC ORANGE 21 DYE BY AN ADSORBENT PREPARED FROM *Adenanthera paronina* L SEEDS

P. Ashokan[1,✉], M. Asaithambi[1], V. Sivakumar[2] and P. Sivakumar[3]
[1]Department of Chemistry, Erode Arts College, Erode, TN, India-638112
[2]Department of Chemistry, Sri Vasavi College, Erode, TN, India-638 316
[3]Department of Chemistry, Arignar Anna Govt Arts College, Namakkal, TN, India-637 002
✉Corresponding Author: ashokanhappygod@gmail.com

ABSTRACT

Adsorption using activated carbon is found to be a promising technology for the removal of dyes present in wastewater. The carbon prepared from *Adenanthera paronina* L seeds (APAC5) through chemical impregnation, microwave carbonization, and finally muffle furnace activation found to have a 948 m^2/g surface area. The microwave heating generates highly branched activated carbon with fewer surface functional groups. The batch mode adsorption of Basic Orange 21 (BO21) dye onto APAC5 is studied. The maximum quantity of BO21 adsorbed is 49.17 mg/g under batch mode study for 50 mg/lof initial BO21 concentration. The nonlinear form of mathematical expression describes the kinetic and isotherm models better under batch mode analysis.

Keywords: Microwave, Chemical Activation, Nonlinear Models, Basic Orange 21, and Batch Mode.
RASĀYAN *J. Chem.*, Vol. 15, No.3, 2022

INTRODUCTION

Water is an essential and integral part of all living things on the planet earth. Textile dyeing industries are the major consumer of fresh water and the major portion of this water is let out as effluent after the completion of the dying process. It is essential to treat the dye-bearing wastewater before discharging them into the environment. The untreated dyeing industry wastewater poses serious implications to the flora and fauna.[1] When these dye molecules enter the human body, they even cause genetic mutations.[2] The complex nature of these organic colorants makes them highly resistant to the existing treatment technologies.[3] There are many treatment methods of physical, chemical, and biological nature that were explored for wastewater purification.[4-6] Adsorption is considered one of the most suitable methods, especially for color removal. Adsorption using high surface activated materials has many advantages like good selectivity towards various category pollutants (anionic, cationic dyes, metal ions, etc.), low operating cost and easy regenerations, etc.[7], Many activated materials like silica[8], clay[9], bentonite[10], silica gel[11], zeolites[12], alumina[13], cellulose[14], chitin[15], bagasse[16] and activated carbon[17,18] are tested for the removal of pollutants from wastewater. During the analysis of an adsorption system, the evaluation of kinetic, and isotherm parameters provide some essential information about the adsorbate-adsorbent interaction, mechanism of adsorption, surface properties, and reaction pathways. A few decades back, computers and data processing software are not available, hence all the mathematical models are linearized and used for data analysis. The data analysis with linear models discards many experimental points which deviate from a straight line to attain a high r^2 value. The results evaluated using linearized mathematical models may be erroneous and may not be the correct ones. On linearizing an inherent nonlinear model without knowing the error structures, the output of the linear model will be erratic. The high r^2 in a linear model does not necessarily mean that the calculated values are true to the experimental value. In order to arrive at a real mechanism of adsorption and also estimate the true results, linear and nonlinear mathematical models are employed for the same adsorption system and the results are compared. Utilization of waste materials from agro wastes for activated carbon preparation can serve many benefits like being economically cheap, most versatile, and easy to regenerate.[19-22] In this study, the seeds of *Adenanthera paronina* L is taken as a raw material for activated char preparation. *Adenanthera paronina* L, it is commonly named red sandal wood, is a tall tree growing in hot and humid regions.[23] Highly porous activated carbon is prepared from the seeds through chemical impregnation. The

http://doi.org/10.31788/RJC.2022.1536782

carbonization is done using a microwave oven after impregnation. The activation of prepared char is performed using a muffle furnace under an inert atmosphere. The high surface activated char is used for the adsorption of Basic Orange 21 (BO21, a cationic dye) through batch mode.

EXPERIMENTAL

Analytical grade chemicals are utilized in this analysis. These chemicals are procured from E. Merck, India are used as received.

A. paronina L Seed Char Preparation

A. paronina seeds collected in Dharmapuri region, Tamilnadu, India. The seeds after collection are washed thoroughly with excess water to remove the adherent impurities followed by drying at 110° C until the complete removal of moisture. The dry seeds are cut into small pieces and soaked in con H_2SO_4 for 24h. After 24h, the solid mass is separated, and the residual acid is completely washed with excess water. The dry residue is heated in a microwave oven at 600w for 10 min. Then the char is repeatedly washed with double distilled water and ground to a particle size of 180 to 300 µ. For the final activation, the char is heated in a muffle furnace under a nitrogen atmosphere at 800° C for 10 min. The resultant activated char (APAC5) is stored in a closed container for further characterization and adsorption analysis.

Surface Characterization of APAC5

To evaluate the types and nature of various surface functional groups present in APAC5, Scanning Electron Microscope (SEM) images are observed. CARL ZEISS make (EVO-18 model) Electron Microscope is utilized for this study. To ascertain the various functional groups present on the activated carbon surface are estimated by recording the IR spectra using FTIR (Perkin Elmer) Spectrophotometer. The BET surface area of the AC's is studied using Quanta chrome Autosorb BET surface area analyzer.

Preparation of Adsorbate

The adsorbate used in this investigation is Basic Orange 21 (BO21) dye (a cationic dye) with a molecular formula $C_{22}H_{23}ClN_2$, Molecular Weight: 351.9 g/mol, C.I. No. 48035 and the maximum absorption wavelength is 492 nm. 1000 mg/l stock dye solution is prepared by adding the appropriate quantity of BO21 dye in double-distilled water. The dye sample purchased for the present study is 98% pure. The stock solution is stored in a refrigerated container to avoid water evaporation. The original stock solution is diluted to the required concentrations with distilled water. The structure of the BO21 dye is given in Fig.-1.

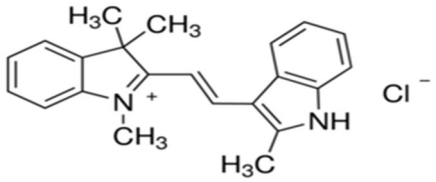

Fig.-1: Structure of Basic Orange 21 (BO21) Dye

Adsorption Studies

All the adsorption experiments are performed by shaking 100ml of dye solution with a known quantity of APAC5 adsorbent. At a specified time interval, an adequate quantity of solution is withdrawn, centrifuged for 4 min (at 5000 rpm) and the remaining BO21 dye concentration is evaluated by recording the absorbance at the λmax of BO21 solution. Systronics make UV-Vis spectrophotometer is used for the estimation of dye concentration as and when required. The following mathematical relations are used for the determination of dye adsorption.

Final residual BO21 concentration in solution (C_t) $= \frac{initial\ OD}{final\ OD}\ x\ C_0$ (mg/L) (1)

Quantity of BO21 dye removed at time t (q_t) = [$C_0 - C_t$] (mg/L) (2)

Quantity of BO21 adsorbed at time t (q_t) = $\frac{[C_0 - C_t]}{quantity\ of\ APAC\ \ per\ litre}$ (mg/g) (3)

Percentage of BO21 dye adsorbed $=\frac{q_t}{C_0}\ x\ 100\ \%$ (4)

Where C_0 is the initial BO21concentration (mg/L) initial OD and final OD are the optical densities of BO21 dye solution prior to and after adsorption experiments. For the kinetic studies, the residual BO21 concentrations are estimated at varying intervals of a time by fixing the initial BO21concentration and temperature as constant. For the isotherm studies, the dye and adsorbent are equilibrated and the final equilibrium dye concentration is calculated at various concentrations under a given set of temperatures.

RESULTS AND DISCUSSION

Surface Characteristics of APAC5

The activated carbon prepared from *A. paronina* seeds was found to have comparable physico-chemical characteristics as shown in Table-1. The APAC5 was prepared by treatment with H_2SO_4, microwave carbonization, and then finally activation in a muffle furnace found to have very low conductivity. The pH of activated carbon is also nearly neutral (6.9). As H_2SO_4 is a powerful charring agent, it removes the majority of the volatile and lignin-related compounds. The carbon surface is free from most of the water and acid soluble impurities as indicated by the low quantity of matter soluble in acid. The microwave carbonization heats the entire material uniformly and produces a highly active and porous carbon with an excellent BET surface area of 948 m^2/g.

Table-1: Some important Characteristics of APAC5

S. No.	Parameter	Value
1.	pH	6.9
2.	Conductivity mS/m^2	0.160
3.	Mater solute in Acid, %	0.72
4.	Moisture content, %	11.3
5.	Volatile matter, %	7.75
6.	Bulk density, g/mL	0.56
7.	Porosity, %	72.45
8.	BET Surface Area, m^2/g	948
9.	Ash, %	10.16

The SEM image of the APAC5 indicates a highly branched carbon network with well-developed porosity. The SEM image of APAC5 is given in Fig.-2a. The SEM image clearly depicts the presence of a huge number of troughs, and crests with plenty of imperfections on the carbon surface. There are plenty of pores of micro, macro, and nano-size observed in the carbon network. The FTIR spectra of APAC5 are shown in Fig.-2b, which can be used to ascertain the functional groups located on the carbon surface. A broad peak confirming the presence of -OH str. (belong to alcohols) is detected from 3400 to 3470 cm^{-1}. As the carbon is a highly porous one, there are plenty of chances for moisture to enter into the pores of carbon, which would have produced the –OH stretching peaks. The -CH str. peaks noted around 2893 to 2924 cm^{-1} demonstrate the existence of an unsaturated carbon network.[24] The CO_2 absorption frequency found in APAC5 at 2426 cm^{-1}, may be occurred due to CO_2 molecules adsorbed by the activated char. The APAC5 shows C=C str. The peak at 1637 cm^{-1} and –CH bending vibrations at 1380 to 1431 cm^{-1}.[25] The presence of a graphitic network having a high degree of unsaturation with a minimum amount of surface functional groups is clearly known from the above peaks[26]. The peak at 1380 to 1384 cm^{-1} responsible for –CH bending of alkenes.[27] The prepared char APAC5 has a superior surface characteristics(based on the FTIR and SEM results). It may give a great result when employed as an adsorbent.

Effect of pH

The charges located on the adsorbent surface are greatly influenced by the solution pH. The chemical structure of the absorbent is changing drastically under different pHs. Most of the dye molecules ionize under the influence of solution pH. The ionized dye molecules interact with an adsorbent in a different manner under different solution pH. The impact of solution pH on the extent of adsorption of BO21 dye is calculated by shaking 100 ml of 50 mg/l dye solution with 100 mg of APAC5. The variation of BO21 adsorption on the APAC5 surface is studied in the pH range of 2 to 11. The percentage of BO21 adsorbed

on APAC5 increased from 64.3% to 98.8% when the pH of the dye solution raised from 2 to 7 as shown in Fig.-3. On further increasing of solution pH, there is a mild reduction in the dye adsorption percentage. From the result, it is inferred that, at lower pH, the surface of the APAC5 is positive, and the positively charged (protonated) APAC5 surface will repel the cationic $[BO21]^+$ dye. As the pH_{ZPC} of APAC5 is 6.7, when the pH of the dye solution goes beyond 6.7, the surface of APAC5 becomes +ve. After the pH of 6.7, the negatively charged APAC5 surface showed great ease of attraction towards $[BO21]^+$.

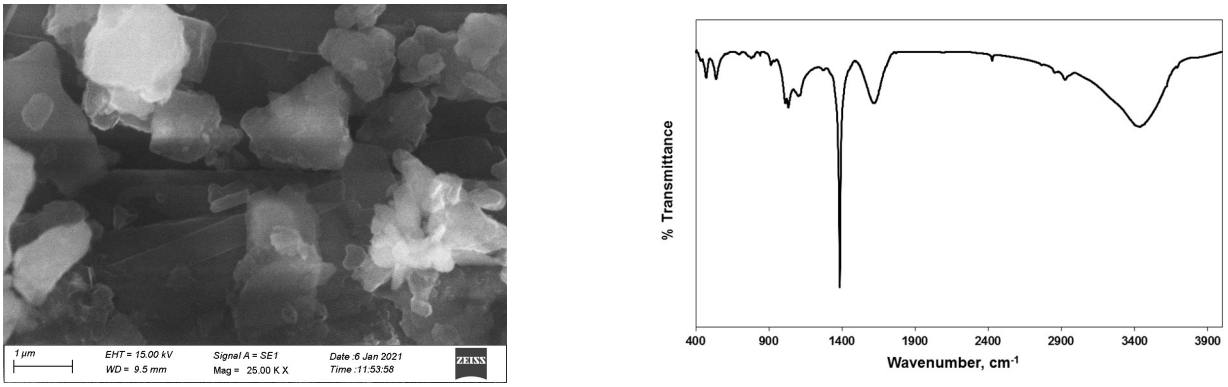

(a) (b)

Fig.-2: (a) SEM and (b) FTIR spectra of APAC5

As the pH of a solution is greater than 8.0, there is a slight reduction in the percentage of BO21 adsorption. At higher pH, the abundant quantity of OH^- ions compete with BO21 dye towards the adsorption sites.[7] Another valid fact that has to be considered here is the pKa of BO21 dye. The pKa of BO21 dye is 4.4 to 5.3, which indicated that the BO21 dye ionizes a reasonable amount and the ion-ion interaction on the APAC5 surface is a significant factor.[28]

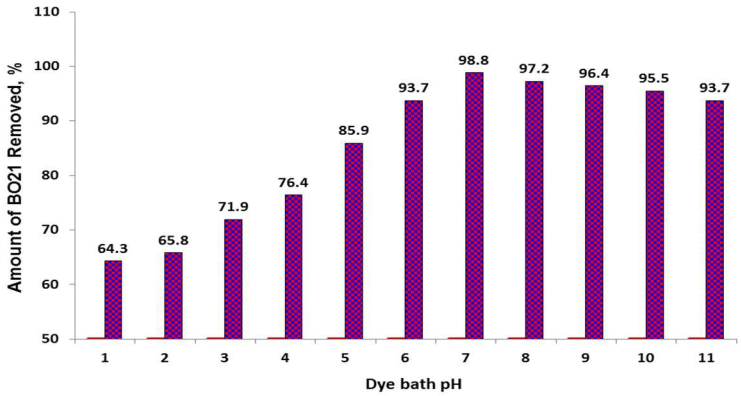

Fig.-3: Variation of BO21 Adsorption as a Function of pH

Effect of Initial BO21 Concentration

The initial concentration of the adsorbate is one of the prime parameter that must be tuned to achieve the maximum efficiency of an adsorbent. The role of initial BO21 concentration on its adsorption is calculated by raising the initial BO21 concentration from 25 to 100 mg/l for fixed dye volume of 100 mL and APAC5 dosage of 100 mg. The variation of percentage and amount of BO21 adsorption onto APAC5 at different initial BO21 concentrations are shown in Fig.-4. When the initial BO21 concentration increased from 25 to 100 mg/L, the BO21 adsorption percentage decreased from 100.0 to 95.29 %, and the amount of BO21 adsorbed increased from 25.0 mg/l to 95.29 mg/l. During the lower concentrations of BO21, the availability of adsorption sites per number of solute molecules is high, hence the dye removal percentage is high. At higher concentrations of BO21, the number of active sites per unit quantity of solute is less and hence the percentage of adsorption shows a decreasing trend. This fact is supported by the result published by Liu *et al.* (2021) for reactive brilliant red K-2G adsorption on PANI-DCC@GO surface.[29]

Effect of Temperature

During the adsorption process, there is some heat exchange is involved in the adsorption system. Depending upon the nature of adsorbent and adsorbate, the heat exchange may be exothermic or endothermic. The role of solution temperature on the adsorption of BO21 onto APAC5 is studied at 30, 35, 40, and 45 °C for an initial BO21 concentration of 50 mg/l as shown in Fig.-5.

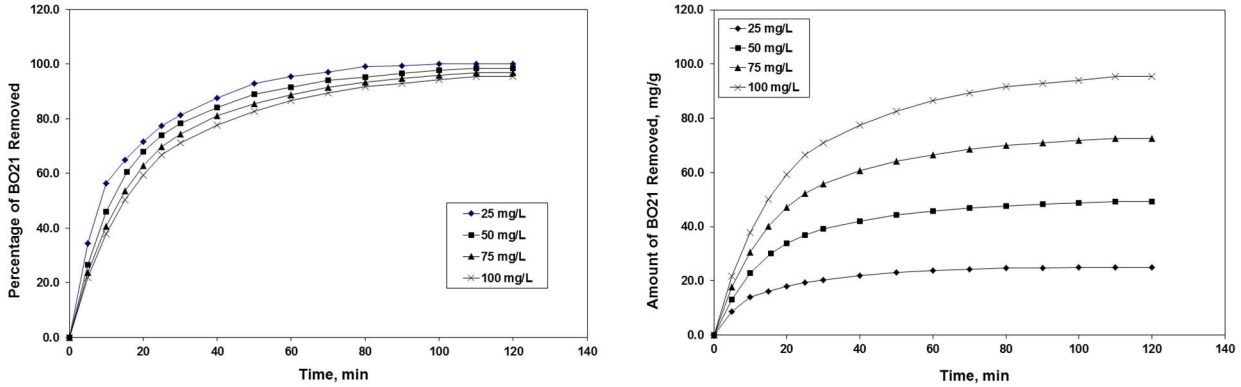

a) b)

Fig.-4: BO21 Dye Adsorption as a Function of Initial Concentration a) Percentage of Adsorption b) Amount of Adsorption

The removal efficiency of BO21 decreased from 98.33 % to 92.86 % on increasing the temperature from 30 to 45°C. The results substantiate that low temperature favors the BO21 adsorption onto APAC5. The trend depicts the exothermic nature of adsorption. At higher temperatures, the kinetic energy and vibrational energy of BO21 molecules increase, which leads to more amount of desorption. Though the quantity of BO21 adsorbed on APAC5 decreased with an increase in temperature, the extent of the decrease is very marginal only. The marginal change in adsorption depicts that there is a small energy change involved for every 5°C rise in temperature.

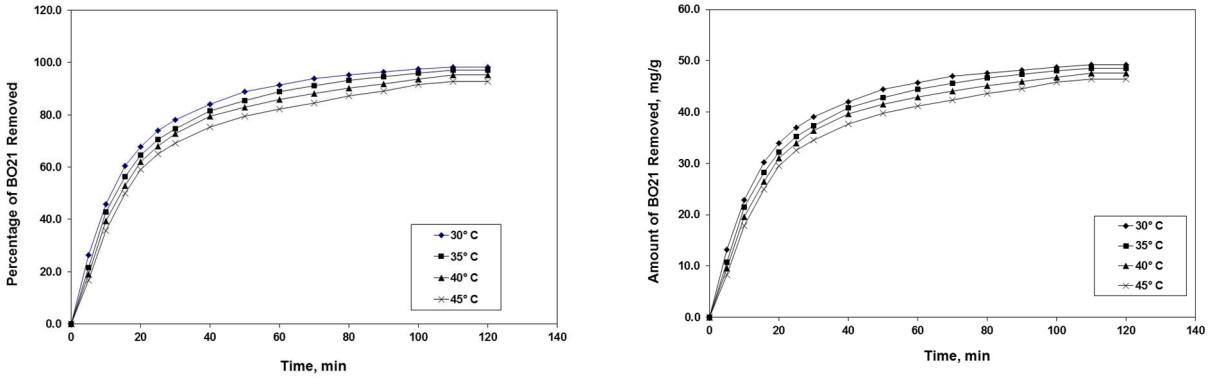

(a) (b)

Fig.-5: BO21dye Adsorption as a Function of Temperature (a) Percentage of Adsorption (b) Amount of Adsorption

Adsorption Kinetics

The pseudo-first-order kinetic expression proposed by Lagergren (1898) is used for the evaluation of adsorption kinetics.[30] In this expression the rate-determining step of adsorption is first-order based on the concentration of adsorbate.[30] The linear and nonlinear form of pseudo-first-order expression is given in equation (5) and (6) respectively.

$$\ln(q_e - q_t) = lnq_e - k_1 * t \quad (5)$$

$$q_t = q_e(1 - exp^{-k_1 t}) \quad (6)$$

Where, q_e is the amount of BO21 adsorbed per unit mass of APAC5 at equilibrium and k_1 is the pseudo-first-order rate constant.

The pseudo-second-order kinetic expression is employed in cases where the pseudo-first-order kinetic model not fit enough.[31] The linear and nonlinear form of pseudo-second-order kinetic expression is given in equation (7) and (8) respectively.

$$\frac{t}{q_t} = \frac{1}{k_2 q_e^2} + \frac{1}{q_e} * t \quad (7)$$

$$q_t = \frac{k_2 q_e^2 t}{1 + k_2 q_e t} \quad (8)$$

Where, k_2 is the pseudo-second-order rate constant and q_e is the equilibrium adsorption quantity calculated using the pseudo-second-order model. The linear and nonlinear plots of pseudo-first-order and pseudo-second-order expressions are shown in Fig.-6 and 7 respectively. The results calculated using linear and nonlinear expressions are provided in Table-2.

Table-2: Results of Kinetic Studies

	Linear Models				Non-Linear Models				Linear Models				Non-Linear Models			
Parameters	Initial dye concentration, mg/L								Temperature °C							
	25	50	75	100	25	50	75	100	30° C	35° C	40° C	45° C	30° C	35° C	40° C	45° C
$q_e$exp.(mg/g)	25.00	49.17	72.62	95.29	25.00	49.17	72.62	95.29	49.17	48.55	47.62	46.43	49.17	48.55	47.62	46.43
Pseudo-first order kinetics																
k_1 (min^{-1})	0.0520	0.0438	0.0396	0.0408	0.0708	0.0606	0.0529	0.0487	0.0438	0.0401	0.0380	0.0364	0.0606	0.0552	0.0525	0.0492
$q_e$cal(mg/g)	21.75	41.66	61.63	88.49	24.42	48.00	71.15	93.62	39.37	41.66	40.83	42.18	48.00	47.32	46.28	45.08
R^2	0.9878	0.9875	0.9933	0.9938	0.9864	0.9951	0.9967	0.9967	0.9928	0.9881	0.9802	0.9693	0.9951	0.9947	0.9950	0.9933
Sd	1.029	2.374	3.475	2.151	0.182	0.368	0.464	0.531	3.097	2.179	2.146	1.344	0.368	0.390	0.423	0.427
R.C.Sq	1.058	5.638	12.073	4.628	1.023	1.523	2.340	4.136	9.591	4.750	4.606	1.806	1.523	1.662	1.531	2.009
R^2 adj	0.9851	0.9847	0.9918	0.9924	0.9833	0.9940	0.9960	0.9960	0.9912	0.9855	0.9758	0.9625	0.9940	0.9936	0.9939	0.9918
Pseudo-second order kinetics																
k_2 (g/mg/min)	0.0036	0.0014	0.0008	0.0005	0.0035	0.0013	0.0007	0.0005	0.0014	0.0011	0.0010	0.0009	0.0013	0.0012	0.0011	0.0010
$q_e$cal(mg/g)	27.47	55.25	83.33	111.11	27.65	55.60	83.96	111.82	55.25	55.56	55.25	54.64	55.60	55.61	54.88	54.02
R^2	0.9995	0.9992	0.9991	0.9991	0.9984	0.9974	0.9980	0.9983	0.9992	0.9982	0.997	0.9954	0.9974	0.9961	0.9948	0.9940
Sd	0.782	1.923	3.388	5.002	0.838	2.035	3.586	5.225	1.923	2.215	2.413	2.598	2.035	2.232	2.295	2.401
R.C.Sq	0.611	3.699	11.480	25.018	0.1188	0.7989	1.4189	2.1240	3.699	4.908	5.821	6.751	0.7989	1.2189	1.6173	1.8059
R^2 adj	0.9994	0.9990	0.9989	0.9989	0.9981	0.9969	0.9976	0.9979	0.9990	0.9978	0.9963	0.9944	0.9969	0.9953	0.9936	0.9926

In case of nonlinear expressions, the experimental q_t fitted to q_t calculated using a nonlinear expression with the help of the Excel Solver Tool. The data process using Excel solver is performed through curve fitting. During curve fitting, q_e and k_1 or k_2 are altered until to achieve a minimum standard deviation (Sd). On analyzing the results given in Table-2, it is inferred that the pseudo-first-order rate constant varied inconsistently under the linear model and it decreased from 7.08 x 10^{-2} to 4.87 x 10^{-2} min^{-1} when the BO21 concentration increased from 25 to 100 mg/l in the case of nonlinear analysis.

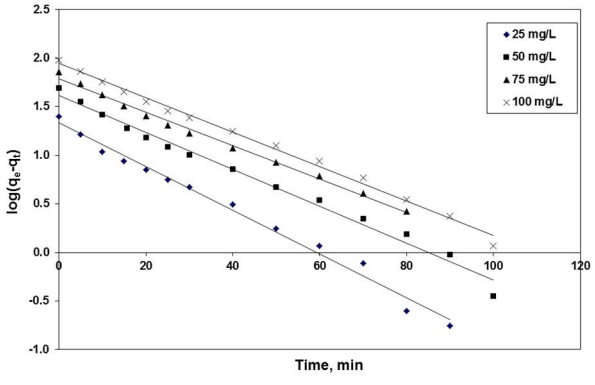

(a)

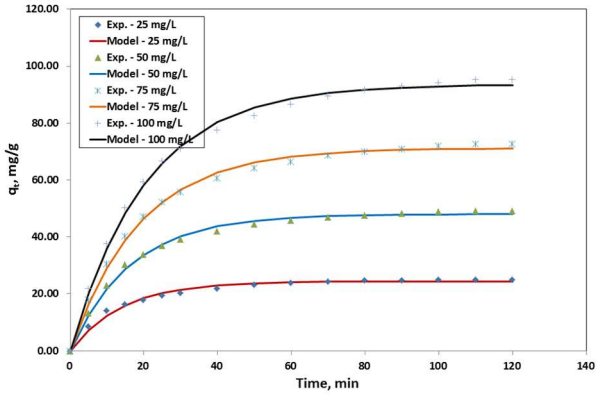

(b)

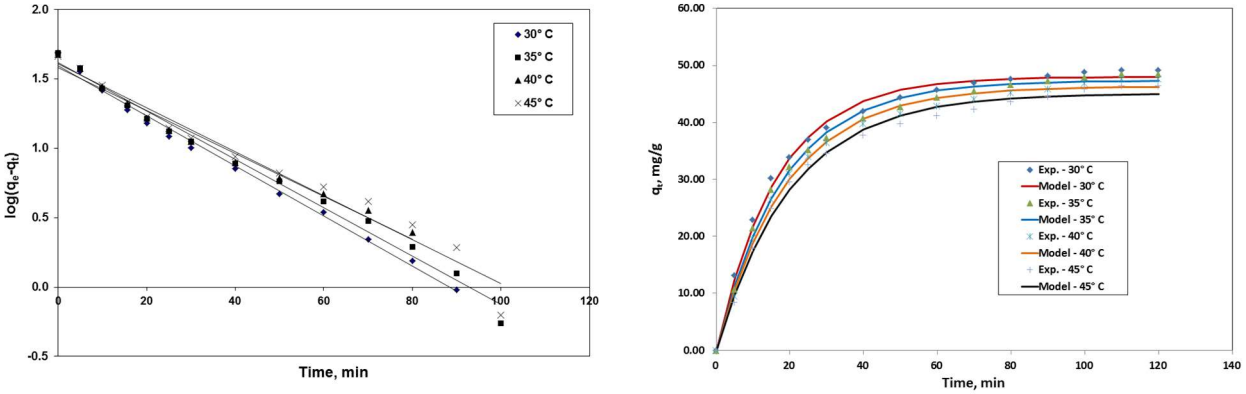

(c) (d)

Fig.-6: Pseudo-First-order Plot a) Linear Plot – Concentration Variation b) Nonlinear Plot – Concentration Variation c) Linear Plot – Temperature Variation d) Nonlinear Plot – Temperature Variation

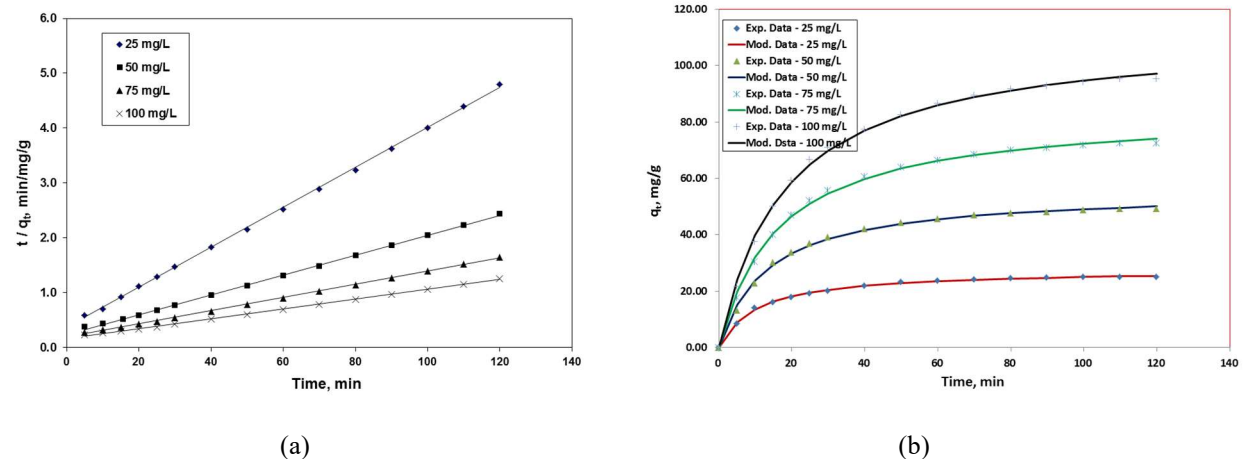

(a) (b)

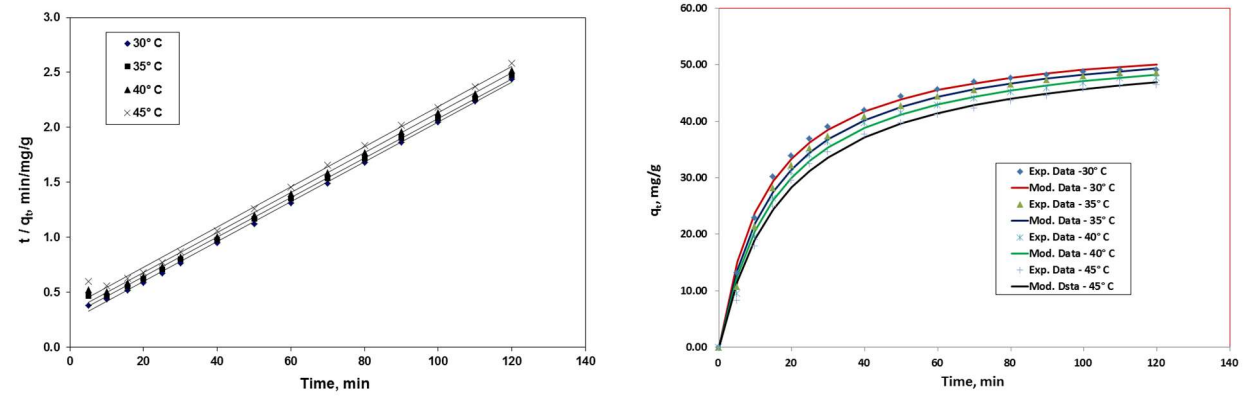

(c) (d)

Fig.-7: Pseudo-Second-Order Plot (a) Linear Plot – Concentration Variation (b) Nonlinear Plot – Concentration Variation (c) Linear Plot – Temperature Variation (d) Nonlinear Plot – Temperature Variation

The value of k_1 calculated using the nonlinear model decreased from 6.06 x 10^{-2} to 4.92 x 10^{-2} min^{-1} on raising the solution temperature from 30 to 45° C. The $q_{e(cal)}$ estimated using a linear model show a high deviation from the experimentally estimated $q_{e(exp)}$. The deviation in q_e is expressed in terms of Sd. The linear model showed high Sd under varying concentrations and temperature (3.475 > Sd > 1.028). The q_e

evaluated using the linear expression under various concentrations and temperature shows a low standard deviation (0.531 > Sd > 0.182).

The pseudo-second-order model is also used to treat the adsorption kinetics where the pseudo-first-order kinetic model fails. In this study, the experimental data is also tested using the pseudo-second-order kinetic expression in linear and nonlinear forms. Like the majority of the results published in the past, this study also showed that the linearized pseudo-second-order model is the best fit with high r^2 ($0.999 > r^2 > 0.9954$) when compared to the pseudo-first-order kinetic model. Analysis of the Sd obtained from the linear model also showed that the pseudo-second-order model is best suited for BO21 adsorption onto APAC5. On looking at the nonlinear model result, the pseudo-first-order model shows minimum Sd when compared to the pseudo-second-order model. According to Lima *et al.* (2015), the prediction of a good kinetic model could not be done based on r^2 only.[32] Multiparameter equations in linear form exhibit r^2 values closer to 1. In such cases, the best fitting model can be predicted based on the r^2_{adj} value only.[33] Based on the above recommendations, the nonlinear form of the pseudo-first-order kinetic model is more appropriate to evaluate the kinetics of BO21 adsorption onto APAC5 (low Sd and high r^2_{adj}).

Isotherm Analysis

The relationship between the quantities of adsorbate on sorbent surface with that of adsorbate in solution at constant temperature is termed as adsorption isotherm. The results of these isotherm models are necessary to understand the nature of the sorbent surface, the type of interaction between adsorbent/adsorbate, and the mechanism of adsorption. The adsorption of BO21 onto APAC5 is evaluated using Langmuir (1918) and Freundlich's (1906) adsorption isotherms.[34,35] The Langmuir isotherm is developed based on the assumptions of monolayer adsorption of adsorbate on an energetically homogenous sorbent surface. The linear and nonlinear form of Langmuir isotherm is given in equations (9) and (10) respectively.

$$\frac{C_e}{q_e} = \frac{1}{Q_0.b_L} + \frac{C_e}{Q_0} \tag{9}$$

$$q_e = \frac{Q_0.b_L.C_e}{(1+b_L.C_e)} \tag{10}$$

The linear and nonlinear Langmuir plot for the adsorption of BO21 onto APAC5 is shown in Fig.-8 and the results are provided in table-3. The Langmuir monolayer adsorption capacity calculated using a linear plot (Q_o) decreased from 192.31 to 109.89 mg/g and it increased from 120.51 to 135.54 mg/g in the nonlinear curve fitting method. Similarly, the Langmuir rate constant (b_L) calculated in the linear model increased from 5.2 x 10^{-3} to 8.8 x 10^{-3} l/mg and it decreased from 9.504 x 10^{-1} to 1.516 x 10^{-1} L/mg in the nonlinear model while increasing the temperature form 30 to 45 ºC.

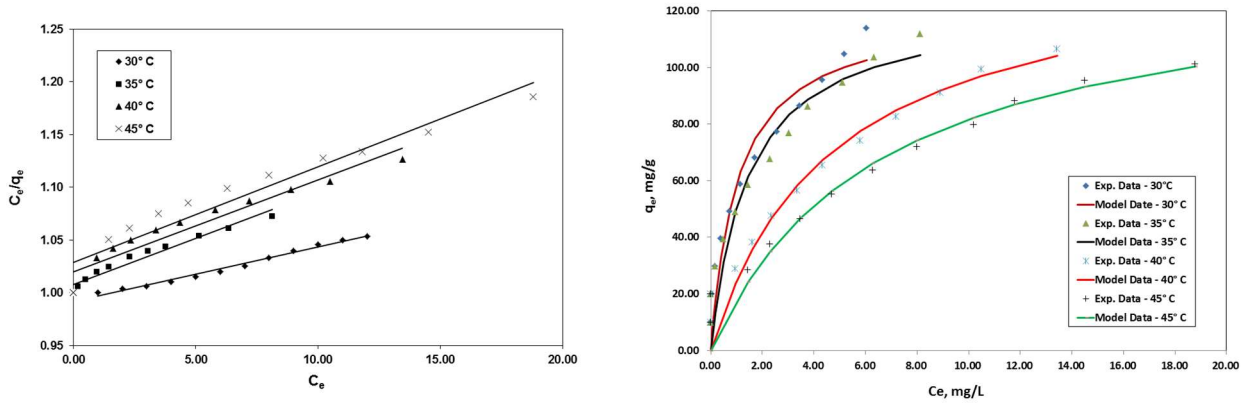

(a) (b)

Fig.-8: Langmuir Plot (a) Linear Plot (b) Nonlinear Plot

Table-3: Results Derived From the Isotherm Plots

Parameters	Linear Model				Nonlinear Model			
	Temperature °C				Temperature °C			
	30	35	40	45	30	35	40	45
1/T, K^{-1}	0.00330	0.00325	0.00319	0.00314	0.00330	0.00325	0.00319	0.00314
Langmuir isotherm								
Q_0 (mg/g)	192.31	128.21	114.94	109.89	120.51	122.84	141.06	135.54
b_L (L/mg)	0.0052	0.0077	0.0085	0.0088	0.9504	0.6927	0.2103	0.1516
r^2	0.9875	0.9569	0.9207	0.9213	0.9402	0.9159	0.9488	0.9451
Sd	--	--	--	--	9.192	10.737	7.959	7.830
R. C Sq	--	--	--	--	84.499	115.283	63.340	61.314
R^2_{adj}	--	--	--	--	0.9252	0.8949	0.9360	0.9314
Freundlich isotherm								
n	2.643	2.511	1.765	26.841	2.695	2.578	2.085	2.099
k_f ($mg^{1-1/n}$ $L^{1/n}$ g^{-1})	55.578	46.709	26.841	0.955	33213.5	38079.1	1341.4	949.6
r^2	0.9987	0.7259	0.9553	0.9245	0.9992	0.9965	0.9961	0.9954
Sd	--	--	--	--	1.085	2.205	2.208	2.256
R. C Sq	--	--	--	--	1.177	4.861	4.875	5.088
R^2_{adj}	--	--	--	--	0.9990	0.9956	0.9951	0.9943

The linear and nonlinear form of Freundlich adsorption isotherm is given in equations (11) and (12) respectively and the plots are shown in Fig.-9.

$$\log q_e = \log k_f + \frac{1}{n}\log C_e \quad (11)$$

$$q_e = k_f C_e^{1/n} \quad (12)$$

On analyzing the results of the Freundlich model in linear and nonlinear expressions, the Freundlich parameter related to the adsorption intensity (n) shows an inconsistent variation in the linear plot and it decreased from 2.895 to 2.099 under nonlinear curve fitting analysis. The value of n varied between 1 to10 under nonlinear expression; whereas it goes beyond 10 under linear plot. The present adsorption system (adsorption of BO21 onto APAC5) shows a good correlation with the Freundlich model.

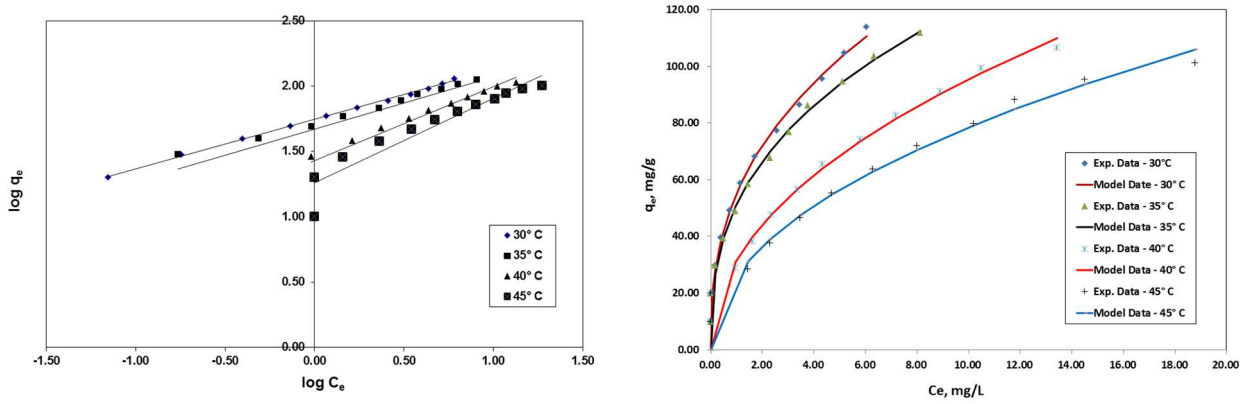

(a) (b)

Fig.-9: Freundlich Plot a) Linear Plot b) Nonlinear Plot

In the case of linear plot analysis, only the r^2 value determines the degree of fitness of a particular model for the selected adsorption system. Generally, in the linear plot, many experimental points are omitted and finally it gives r^2value close to 1.0. The multi-parameter mathematical models like Freundlich and Langmuir isotherm models, the transformation to linear expression may give some errors in the computed results. In the case of mathematical models with more than two parameters, it is essential to evaluate the Sd and r^2_{adj} to determine the fitness instead of r^2 values alone. Based on the above fact that the Sd and r^2_{adj} were computed in nonlinear curve fitting models. The low Sd and high r^2_{adj} is obtained for Freundlich

adsorption isotherm model ($0.9900 < r^2_{adj} < 0.9956$, $1.085 < Sd < 2.256$). This result validates that the BO21 adsorption on APAC5 occurs as a multilayer, the surface of APAC5 is energetically heterogeneous and the concentration of BO21 on APAC5 increases linearly with an increase in BO21 concentration. The magnitude of adsorption favorability (n) evaluated from the Freundlich nonlinear curve fitting analysis indicates that the adsorption of BO21 onto APAC5 is favorable and promising one.

Adsorption Thermodynamics

The amount and nature of heat transformation during the adsorption, spontaneity, and feasibility of BO21 adsorption onto the APAC5 are evaluated using the following equations:

$$\Delta G^\circ = -RT \ln k_L \quad (13)$$

$$\Delta G^o = \Delta H^\circ - T\Delta S^\circ \quad (14)$$

Where, $k_L = M_{BO21} \times b_L$, b_L is the Langmuir constant, M_{BO21} is the molecular weight of BO21 dye. A plot of 1/T vs $\ln k_L$ gives a linear trace with $\Delta H^\circ/2.303$ R as slope and $\Delta S^\circ/2.303$ R as intercept. The results of the thermodynamic analysis are provided in Table-4.

Table-4: Thermodynamic Parameters of BO21 Adsorption

Temperature °C	ΔG°	ΔH°	ΔS°
30	-13.23	- 27.54	93.97
35	-12.45		
40	-12.39		
45	-12.30		

According to Liu (2009), when the dye concentration is definite, it is essential to multiply the molecular weight of BO21 dye with b_L to get the error-free ΔG° value.[36] The negative Gibbs free energy change represents that the adsorption of BO21 by APAC5 is feasible and spontaneous in nature.[37] The more negative value of ΔG° at lower temperature demonstrates that higher temperature is not favored for BO21 adsorption. The negative sign of ΔH° shows the exothermic nature involved during BO21 adsorption which has proved experimentally by the decreased value of q_e at higher temperatures. The entropy (ΔS°) is an indication of the degree of randomness in the adsorption system. When the adsorption proceeds towards equilibrium; the randomness of the system decreases and the orderliness increases as seen from the positive ΔS^o value.

CONCLUSION

Activated carbon with well-developed porosity and excellent surface area is prepared from *A. paronina* seeds, Basic pH seems a better medium for high adsorption of BO21 dye onto APAC5. The amount of BO21 adsorbed is increased from 25.00 to 95.29 mg/g when the BO21 concentration is raised from 25 to 100 mg/l. The decreased adsorption with raise in temperature indicates the exothermic nature. Nonlinear curve fit analysis demonstrates that pseudo-first-order kinetic and Freundlich type of isotherm is obeyed. The APAC5 has good recyclability shows APAC5 is a potential sorbent for BO21 dye adsorption.

REFERENCES

1. P. E. Dim, *Academic Research International*, **4**, 330 (2013).
2. S. Popli and U.D. Patel, *International Journal of Environmental Science and Technology*, **12**, 405(2015), https://doi.org/10.1007/s13762-014-0499-x
3. T. Liu, Z. Wang, X. Wang, G. Yang and Y. Liu, *International Journal of Biological Macromolecules*, **182**, 492(2021), https://doi.org/10.1016/j.ijbiomac.2021.04.038
4. Q.M. Kong, X.J. Wang and T. Lou, *Carbohydrate Polymers*, **244**, 116481(2020), https://doi.org/10.1016/j.carbpol.2020.116481
5. X.Q. Liu and L. Cai, *Applied Surface Science*, **483**, 875(2019), https://doi.org/10.1016/j.apsusc.2019.03.273
6. P.V. Nidheesh, M.H. Zhou and M.A. Oturan, *Chemosphere*, **197**, 210(2018), https://doi.org/10.1016/j.chemosphere.2017.12.195

7. S. Hussain, M. Kamran, S. A. Khan, K. Shaheen, Z. Shah, H. Suo, Q. Khan, A. B. Shah, W. U. Rehman, Y. O. Al-Ghamdi and U. Ghani, *International Journal of Biological Macromolecules*, **168**, 383(2021), https://doi.org/10.1016/j.ijbiomac.2020.12.054
8. G. McKay and M.S. Otterburn, A.G. Sweeney, *Water Research*, **15(3)**, 327(1981), https://doi.org/10.1016/0043-1354(81)90036-1
9. F. Sejie and M. N. Tabbiruka, *Physical Chemistry*, **6(2)**, 39(2016), https://doi.org/10.5923/j.pc.20160602.02
10. Q.H. Hu, S.Z. Qiao, F. Haghseresht, M.A. Wilson and G.Q. Lu, *Industrial & Engineering Chemistry Research,* **45(2)**, 733(2006), https://doi.org/10.1021/ie050889y
11. J. Lin, J.A. Siddiqui and R.M. Ottenbrite, *Polymers for Advanced Technologies*, **12**, 285(2001), https://doi.org/10.1002/pat.64
12. M. Rahmani and M. Sasani, *Journal of Applied Chemistry*, **11**, 83(2017).
13. B. Shi, G. Li, D. Wang, C. Feng and H. Tang, *Journal of Hazardous Materials*, **143(1–2)**, 567(2007), https://doi.org/10.1016/j.jhazmat.2006.09.076
14. G. Zhang, L. Yi, H. Deng and P. Sun, *Journal of Environmental Science*, **26(5)**, 1203(2014), https://doi.org/10.1016/S1001-0742(13)60513-6
15. G. Akkaya, İ. Uzun and F. Güzel, *Dyes and Pigments*, **73**, 168(2007), https://doi.org/10.1016/j.dyepig.2005.11.005
16. H. D. Utomo, N. Phoon, Z. Shen, L. Ng and Z. Lim, *Natural Resources Forum*, **6**, 209(2015), https://doi.org/10.4236/nr.2015.64019
17. Z. Hu and M. Srinivasan, *Microporous Mesoporous Materials*, **43,** 267(2001), https://doi.org/10.1016/S1387-1811(00)00355-3
18. N.F. Cardoso, E.C. Lima, B. Royer, M.V. Bach, L.A.P.G.L. Dotto and T. Calvete, *Journal of Hazardous Materials*, **241**, 146(2012), https://doi.org/10.1016/j.jhazmat.2012.09.026
19. Y. K. Meshram, R. U. Khope and P. P. Chahande, *Rasayan Journal of Chemistry*, **13(4)**, 2302(2020), http://dx.doi.org/10.31788/RJC.2020.1345752
20. T.Y. Kim, I.H. Baek, Y.D. Jeoung and S.C. Park, *Journal of Industrial and Engineering Chemistry*, **9**, 254(2003),
21. G. Sreelatha, P. Srineetha, M. V. S. M. Reddy and K. Ravindhranath, *Rasayan Journal of Chemistry*, **13(4)**, 2230 (2020), http://dx.doi.org/10.31788/RJC.2020.1345997
22. Mariana, F. Mulana , D. N. Pratama and S. Muchtar, *Rasayan Journal of Chemistry*, **13(4)**, 2413(2020), http://dx.doi.org/10.31788/RJC.2020.1346006
23. P. Ashokan and M. Asaithambi, *Journal of Applicable Chemistry*, **8**, 259(2019),
24. N.S.A. Mubarak, A.H. Jawad, W.I. Nawawi, *Energy Ecology and Environment*, **2**, 85(2017), https://doi.org/10.1007/s40974-016-0027-6
25. E.C. Lima, B. Royer, J.C.P. Vaghetti, N.M. Simon, B.M. da Cunha, F.A. Pavan, E.V. Benvenutti, R. Cataluña-Veses and C. Airoldi, *Journal of Hazardous Materials*, **155**, 536(2008), https://doi.org/10.1016/j.jhazmat.2007.11.101
26. P.N. Palanisamy and P. Sivakumar, *Desalination*, **249**, 388(2009), https://doi.org/10.1016/j.desal.2009.09.006
27. Z. Qi, Q. Liu, Z. Zhu, Q. Kong, Q. Chen, S. Zhao, Y. Liu, M. Miao and C. Wang, *Desalination and Water Treatment*, **57**, 29421(2016), https://doi.org/10.1080/19443994.2016.1198929
28. G.B.B. Varadwaj, S. Rana, K. Parida and B.B. Nayak, *Journal of Materials Chemistry A*, **2(20)**, 7526(2014), https://doi.org/10.1039/C4TA00042K
29. Y. Liu and Y.J. Liu, *Separation and Purification Technology*, **61**, 229(2008), https://doi.org/10.1016/j.seppur.2007.10.002
30. S. Lagergren, *Kung Sven Veten Hand*., **24**, 1(1898).
31. Y.S. Ho and G. McKay, *Process Biochemistry*, **34**, 451(1999), https://doi.org/10.1016/S0032-9592(98)00112-5
32. E. C. Lima, M.A. Adebayo and F.M. Machado(2015), Kinetic and Equilibrium models of adsorption. In: Bergmann CP, Machado FM (eds) Carbon nanomaterials as adsorbents for environmental and

biological applications, 1st edn. Springer, New York, pp 33–69, https://doi.org/10.1007/978-3-319-18875-1_3
33. M.A. Adebayo, L.D.T. Prola, E.C. Lima, et al., *Journal of Hazardous Materials*, **268**, 43(2014), https://doi.org/10.1016/j.jhazmat.2014.01.005
34. Langmuir, *Journal of American Chemical Society*, **38**, 2221(1918), https://doi.org/10.1021/ja02254a006
35. H. Freundlich, *Journal of Physical Chemistry*, **57**, 387(1906).
36. Y. Liu, *Journal of Chemical & Engineering Data*, **54**, 1981(2009), https://doi.org/10.1021/je800661q
37. F. Cicek, D. Ozer, A. Ozer and A. Ozer, *Journal of Hazardous Materials*, **146**, 408(2007), https://doi.org/10.1016/j.jhazmat.2006.12.037

[RJC-6782/2021]